



Article Processing Dates: Received on 2023-06-24, Reviewed on 2023-08-04, Revised on 2023-10-03, Accepted on 2024-01-25 and Available online on 2024-02-29

Safety Analysis Factor Of Smart Shredder Machine Frame For Face Mask Waste

Hendi Lilih Wijayanto^{1*}, Amiruddin¹, Angga Tegar Setiawan¹, Yusdianto², Joko Sulisty³

¹Department of Mechanical Maintenance Engineering, Politeknik Industri Logam Morowali, Morowali, 94974, Indonesia

²Department of Mineral Chemical Engineering, Politeknik Industri Logam Morowali, Morowali, 94974, Indonesia

³Department of Electrical and Installation Engineering, Politeknik Industri Logam Morowali, Morowali, 94974, Indonesia

*Corresponding author: hendilw@gmail.com

Abstract

The COVID-19 pandemic emerged as a global public health threat. Hence, the potential danger increased the use of health masks, resulting in increased medical waste in the environment. This incident also occurred in Morowali District, especially in the PT Indonesia Morowali Industrial Park area. The waste produced by employees was disturbing; thus, it required urgent prevention and control of a pandemic. During the pandemic, the industrial area (IMIP) needed to provide various health protocol facilities that directly/indirectly benefited employees' health. This research designed a tool to solve this problem, namely the frame design of the smart shredder machine for face mask waste. This device works automatically (IOT) to shred, process, and sterilize mask waste. The results of this tool can be monitored through periodic applications for the mask waste sterilization system and the destroyed mask waste storage system. This tool is suitable for placing in high-mobility industrial areas, such as the IMIP industrial area, which has around 60,000 employees.

Keywords:

Covid-19, mask waste, smart.

1 Introduction

The emergence of the coronavirus disease (COVID-19) in early December 2019 has attracted attention from around the world[1]. In Wuhan, Hubei Province, China, an acute respiratory syndrome coronavirus two (SARS-CoV-2) occurred[2], the human coronavirus (SARS-CoV-2) and its potential hazards have increased the use of medical masks and waste in the environment, thus requiring urgent pandemic prevention and control. To persuade the waste management and scientific community to find solutions to reduce the harmful consequences of waste disposal, this research estimates the production of medical masks and waste in Asia during the pandemic[3].

World Health Organization (WHO) continues to remind the importance of proper use, storage, and disposal of masks to ensure the best effectiveness of masks and to avoid increasing the risk of disease transmission. The WHO has released recommendations that forbid the reuse of single-use masks [4].

In Indonesia, the COVID-19 disease grew rapidly as it was discovered on April 20, 2021. There were 1,614,849 positive cases of COVID-19[5]. The increase in coronavirus cases has resulted in an increase in the amount of medical waste during COVID-19;

hence, it caused an increase in infectious waste due to COVID-19, which had the potential to harm public health and the environment[6]. Hot weather conditions can cause damage to the mask more quickly due to its sensitivity to heat, and its lifespan is only 72 hours [7]. In addition, according to one research, the COVID-19 virus can survive up to one day on materials such as cloth and wood, two days on surfaces such as glass, four days on materials such as stainless steel and plastic, and up to seven days on the outer layer of surgical masks[8][9].

In closed spaces such as homes, hospitals, and other environments, people are more likely to come into close contact with and transmit the COVID-19 virus[10]. In addition, it is recognized that transmission of COVID-19 can occur in places other than health facilities, such as buildings, places of worship, community centers, markets, public transportation centers, and commercial districts[10][11].

According to Indonesian Institute of Sciences (LIPI) data, during the pandemic, from March to September 2020, Indonesia produced 1,662.75 tons of hazardous and toxic waste (B3), including masks and Personal Protective Equipment (PPE). Since the start of the pandemic in April 2020, more than 1,500 kg of disposable mask waste has been generated by homes only in the capital city of DKI Jakarta[12]. According to research from the University of Massachusetts Lowell and California Baptist University, not using a mask to prevent the spread of the COVID-19 virus could be deadlier. Furthermore, the research published in Physics of Fluids stated that surgical masks with an additional three layers had an efficiency of 65% in filtering airborne particles. However, once used, its potency would drop by 25%[13]. Which in size and design represents his push mower used for mowing strips (roadside) in front of residents' houses with three trials producing the different types of debris, lots of mask waste left in the yard after each cutting[14].

In 2019, Akhil Sharma and Ashish Kumar made the design and fabrication of surgical masks and gloves.

Shredding machines with the Autocad 2020 application resulted in a machine design with dimensions of 91×60×60 cm through destroying masks manually[15]. The prototypes were still manual for their use and did not develop a sterilization system.

Furthermore, Immanuel Beckham and friends used the reverse engineering method to design a mask crushing machine which was modified with a disinfectant sprayer, and the vdi 2221 machine produced specifications with dimensions of the upper body 8×28.6×7 cm and the lower body 8×28.6×30 cm. The length of the shredder was 12 cm, and the capacity of the disinfectant was 1 liter[16]. However, the drawback of this machine was to shred or use it manually by pressing the power button.

Hence, based on the explanation of existing problems and existing regulations and encouragement from the Moorowali industrial area, equipment that can process the processing and prevent the use of medical mask waste is required. Researchers have created storage bins that could be shredded after cleaning, killing any remaining bacteria with a liquid disinfectant on medical masks to reduce the possibility of spreading the COVID-19 virus.

2 Research Method

Experimental design and procedures were the methods of this research. The experiment started with a literature study, namely looking for existing sources of information. This sub-chapter contains how the experiment applied and designed the tools and materials needed.

2.1 Design Draft

A frame is a flat piece of furniture made of several rods joined at the ends to form a solid frame. The frame of this shredder machine used a hollow size of 4×4cm with a thickness of 2mm. The total dimensions of the frame were 50×43cm with a height of

49cm. The function of the frame in this research was at the top as a motor mount and shredder. At the bottom, it functions as a holder for the mask trash can (Fig. 1 - Fig. 3).

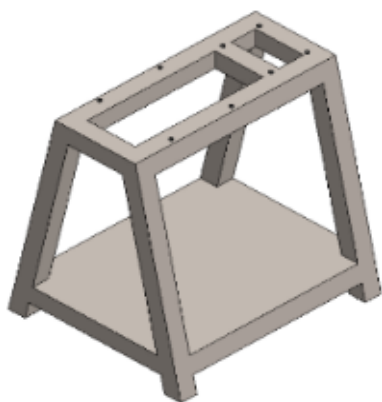


Fig. 1. Frame.

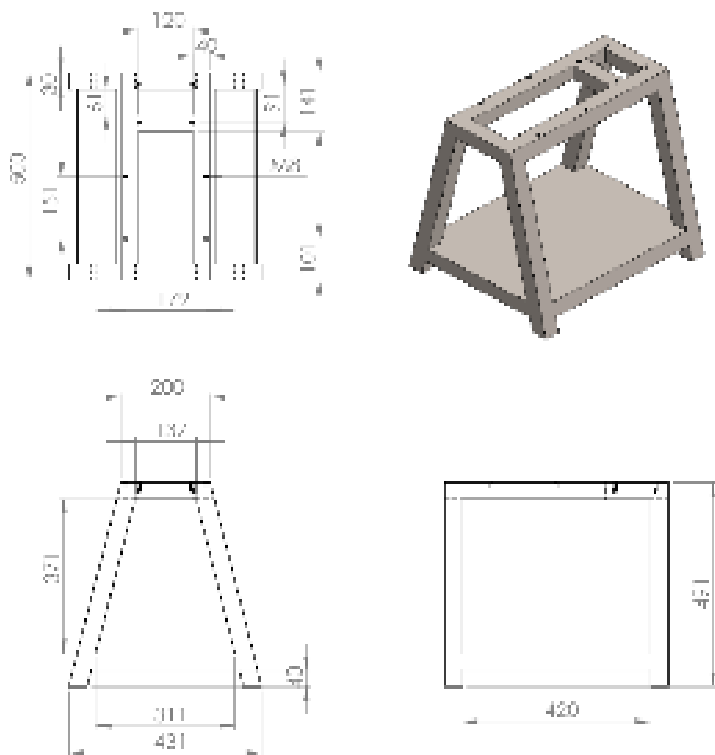


Fig. 2. Detailed frame design.

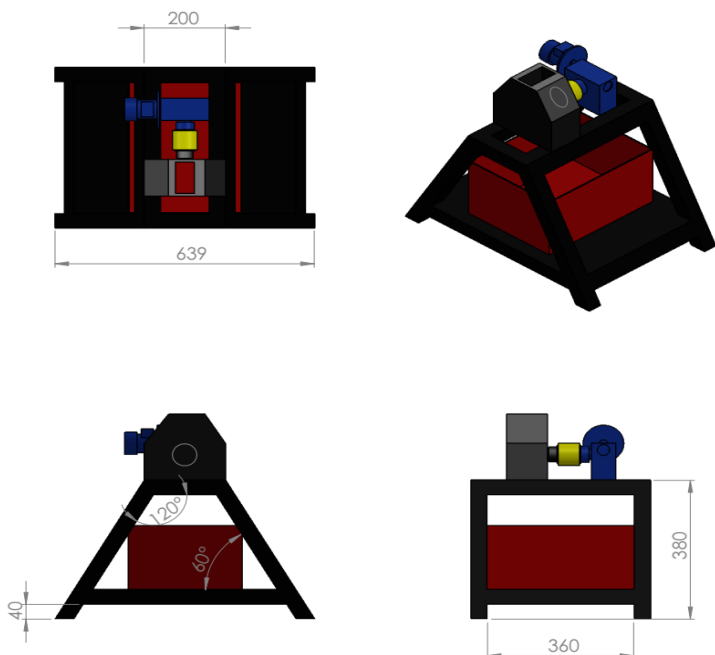


Fig. 3. Design of smart shredder machine for face mask waste.

The design of the frame the trash can and the smart shredder was driven by a 220V AC motor at the top of the trash can. At the top, there is a hole to insert the mask waste. Furthermore, the pit had direct access to the shredder machine; thus, the masks were directly shredded. It went into the dump area, after which it automatically sprayed disinfectant from a disinfectant canister with a capacity of 2 liters. A door might be at the front of the tool; thus, the trash can manager could easily pick up the mask waste.

2.2 Stress and Strain

Stress is the amount of force applied to a unit area[17].It is created by Eq. 1.

$$\text{Stress } (\sigma) = \frac{F}{A} \quad (1)$$

In which:

σ = stress (N/m²)

F = working force (N)

A = area (m²)

2.3 Static Failure Theory and von Mises Stress

Huber introduced the failure theory in 1904, and von Mises and Henky contributed to its development[18]. According to this hypothesis, when the distortion force per unit volume is equal to or greater than the distortion force per unit volume at failure in a direct uniaxial stress test on specimens of the same material origin, failure is projected to occur under multi-axial stress conditions[19] (σ').

The uniaxial tensile stress, which can produce the same deformation energy as that obtained from the combined working stresses, is known as the effective von Mises stress (σ') [20].

2.4 Safety Factor

The factor employed to assess the safety of machine components is called the safety factor. The actual strength of a material must be greater than the strength required to prevent structural failure [21].

The factor of safety is defined as the ratio of required strength (n) to actual strength as follows:

1. Ductile materials

- $\eta = 1.25$ to 2.0 for structural designs with a high degree of confidence for all design data is recommended.
- $\eta = 2.0$ to 2.5 for machine element designs subjected to dynamic loads, the acceptable confidence range for all design data.
- $\eta = 2.5$ to 4.0 for the design of static structures or machine components susceptible to dynamic loading under unknown loads, material characteristics, stress analysis, or the environment.
- 4.0, or more for designing static structures or machine components subjected to dynamic loads with uncertainty regarding particular material combinations, material properties, stress analysis, or the environment.

2. Brittle materials

- $\eta = 3.0$ to 4.0 for structural designs absorbing static load with high confidence for all design data.
- $\eta = 4.0$ to 8.0 for the design of static structures or machine components subjected to dynamic loading with unknown material load, stress analysis, or environmental parameters.

2.5 Static and Dynamic Stresses

A component is said to have passive stress (also known as static stress) when it receives a load applied gradually, without shock, and is held at a constant value. As an illustration, consider the load borne by dead loads on a structure. Forward-moving stresses, such as those in gears and crankshafts, are those produced by forces that change in strength, direction, or both. The allowable static stress is greater than the allowable forward stress due to change[22].

2.6 Solid works Software

The process of designing and assessing structures can be made simpler and easier with the help of Solidworks, which offers integrated solutions. The benefit of an integrated solution is that the entire process can be completed on a single computer running a single piece of software, eliminating the need to move data from one design or computer to another. By using this procedure, data loss or rumors can be prevented, and the analysis process can be accelerated. Analyze structure is done in Solidworks.

2.7 Data Material

The size of the hollow employed in making the frame was 40×40mm with a thickness of 2mm (Fig. 4). Table 1 provides the following information regarding AISI 1015 hollow iron parameters [17].



Fig. 4. Hollow 40×40mm.

The configurate material option in Solid works could be employed to access the entered material data, and the material used was AISI 1015 steel, cold drawn (SS). Material data used included as shown in Table 1.

Table 1. AISI 1015 specifications

Property	Value	Units
Moderate elasticity	2.05E+11	N/m ²
R. Poisson	0.29	N/A
Shear numerus	8.00E+10	N/m ²
Mass density	7870	kg/m ³
The tensile strength	385000000	N/m ²
Lulu strength	325000000	N/m ²
Thermal expansion coefficient	1.20E-05	/K
Thermal conductivity	52	W/(mK)
Specific heat	486	J/(kgK)
Material from dampening ratio		N/A

3 Results and Discussion

3.1 Material Static Analysis Results

Von Mises, displacements, and Factor of Most Secure (FOS) produced on AISI 1015 steel, cold drawn (SS) in the frame analysis of this research used Solidworkssoftware. Fig. 5 illustrates the von Mises material test results on AISI 1015 steel, cold drawn (SS).

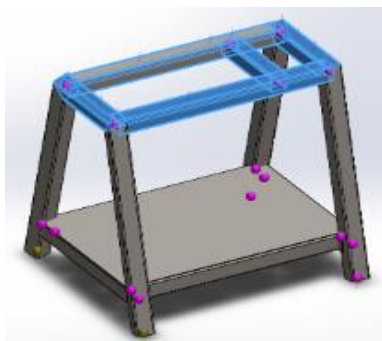


Fig. 5. Field loading point 1.

3.1.1 Loading Frame of Area 1

Four edges were used to apply loading to the surface framing area 1, as illustrated is subject to loading, which is equal to 23.3 kg or 233 N displacement.

Area 1 of the frame was initially subjected to a load of 233 N (23.3 kg.), and using the color diagram of the red area, it could be calculated that the resulting aphorism strain was 5.236e-07 N/m². It was the first known value from simulation studies (Fig. 6).

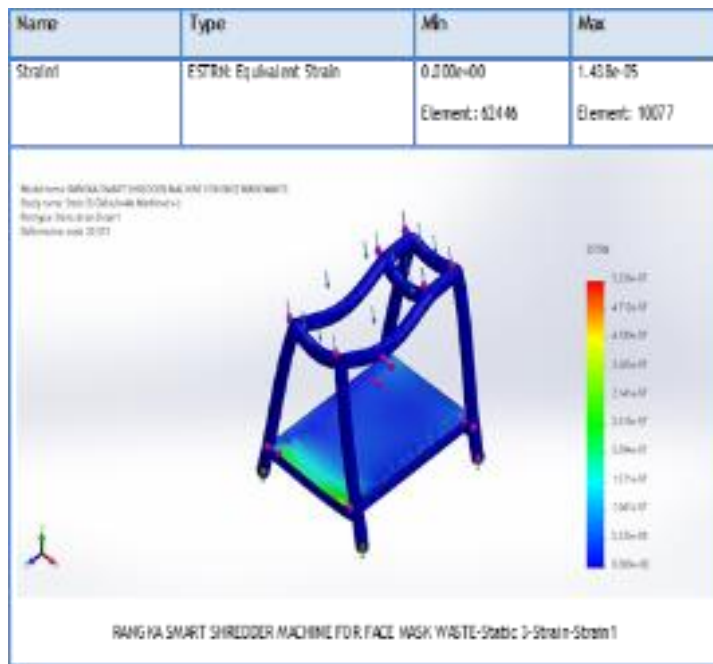


Fig. 6. Results of stress analysis of the loading area of frame 1.

In the recently completed displacement simulation research, the red diagram indicates the maximum displacement value at the loading point of frame area 1 with a value of 2.897e-03 mm (Fig. 7).

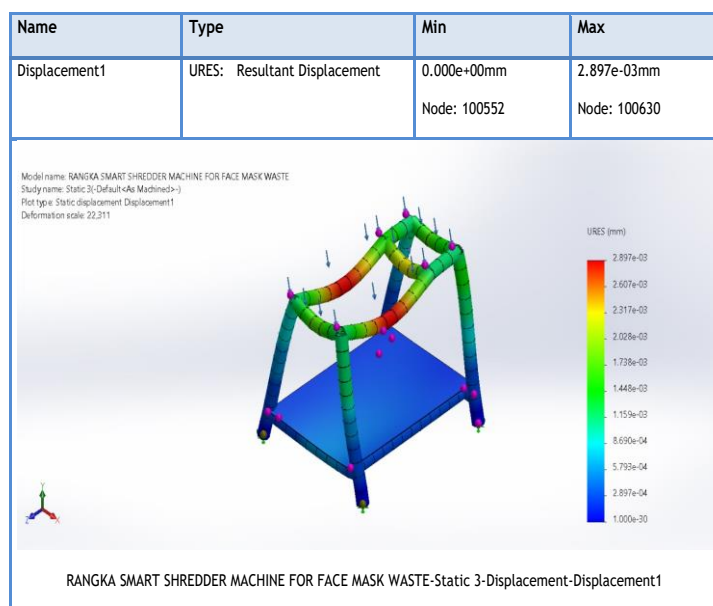


Fig. 7. Displacement analysis results in the loading area of frame 1.

Based on conclusions from the color diagram of the simulation results illustrated in Fig. 8, it is evident from the graph that the maximum stress value or the resulting stress value was 6.117×10⁴ N/m², which indicated that the maximum stress value was still below the yield strength of the material used to make the machine frame.

If it is determined that the loading of the frame is carried out using the area of safety factor 1, the value of the safety factor can be determined using the Eq. 2.

$$Sf = \frac{\sigma_{\text{yield strength}}}{\sigma_{\text{max vonMises}}} \quad (2)$$

$$Sf = \frac{3.25 \times 10^8 \text{ N/m}^2}{6,117 \times 10^4 \text{ N/m}^2}$$

$$= \frac{325.000.000}{61.170}$$

$$= 5.313 \text{ N/m}^2$$

Description:

Safety factor = Sf

Yield strength of the material = σ yield strength

Maximum working stress = σ max von Mises

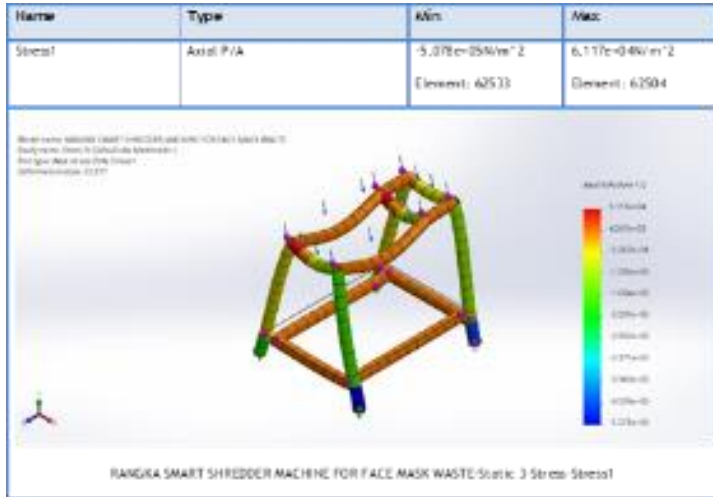


Fig. 8. Result of area 1 frame load stress.

The frame design generated for loading in area 1 was safe to support a load of 233 N (23.3 kg) based on the frame safety factor value results, which exceeded the required value (Fig. 9).

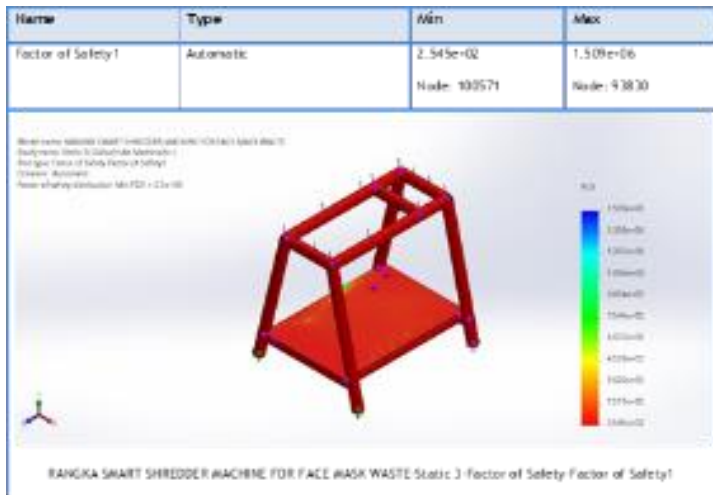


Fig. 9. Safety factor with a load of 17 kg on the frame.

3.1.2 Loading Frame of Area 2

The bottom plate frame was loaded. As could be illustrated in Fig. 10, a load of 5 kg or 50 N was applied to the top.

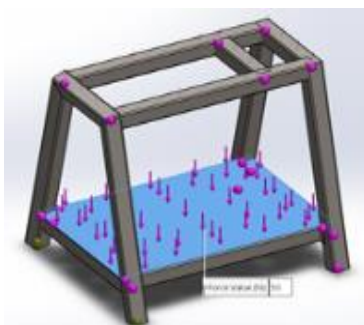


Fig. 10. Loading frame of area 2.

An initial load of 50 N (5 kg) was applied to the frame in area 2, and the maximum possible strain was 6.921e-06 N/m², as illustrated by the color diagram in the red area, the first known value from the simulation analysis (Fig. 11).

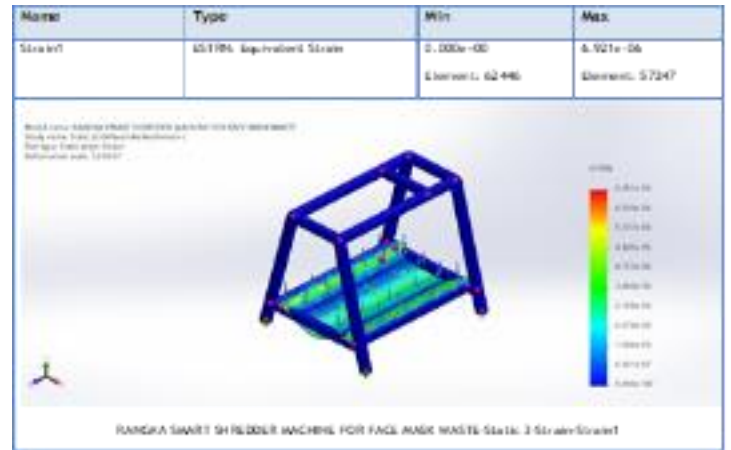


Fig. 11. Results of loading strain analysis for area 2 frame.

In the recently completed displacement simulation research, the red color diagram with a value of 3.432e-02 mm represented the maximum displacement value at frame area 2 loading (Fig. 12).

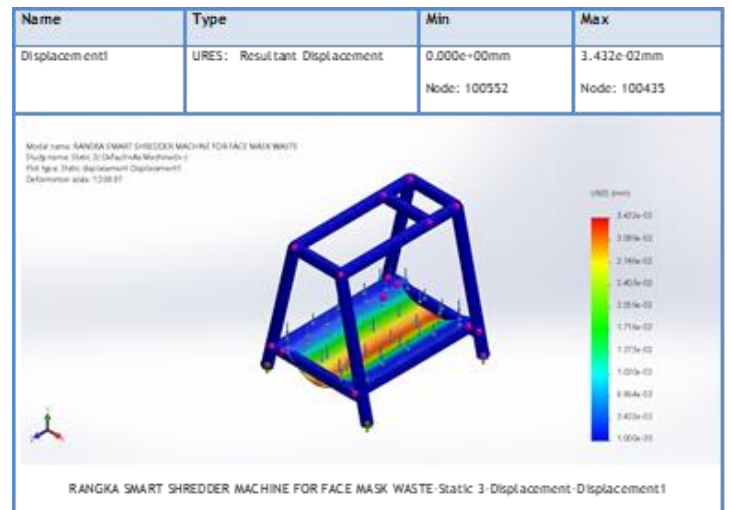


Fig. 12. Displacement analysis results on the frame loading area in the displacement simulation study.

As illustrated from the color diagram of the simulation results in Fig. 13 and can be observed, the maximum stress value achieved was 2.303×10⁶ N/m², which indicated that the maximum stress value was still below the yield strength value of the material used to make the machine frame.

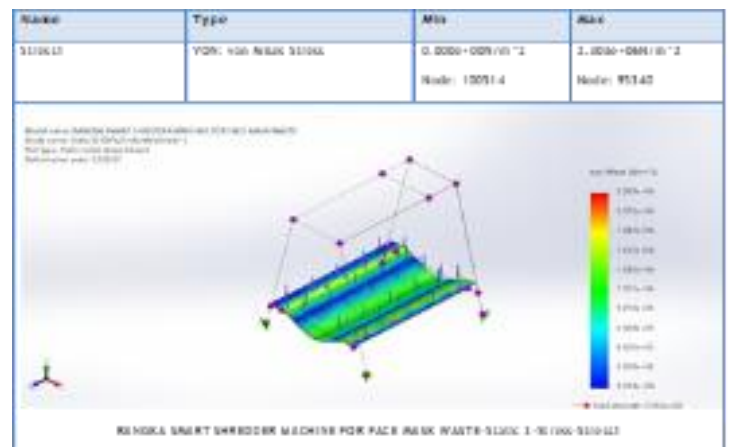


Fig. 13. Result of loading stress in area 2 frame.

With the Eq. 2, the value of the factor of safety could be determined to find out whether the frame loading in area 2 was safe to use.

$$Sf = \frac{\sigma \text{ yield strength}}{\sigma_{\max \text{ vonMises}}}$$

$$Sf = \frac{3.25 \times 10^8 \text{ N/m}^2}{2.303 \times 10^6 \text{ N/m}^2}$$

$$= \frac{325,000,000}{2,303,000}$$

$$= 141 \text{ N/m}^2$$

A load weighing 50 N (5 kg) could be safely supported by a frame made for loading in area 1, according to the findings of the safety factor value of loading the frame in area 2 (Fig. 14). Based on these results, it has exceeded the required value.

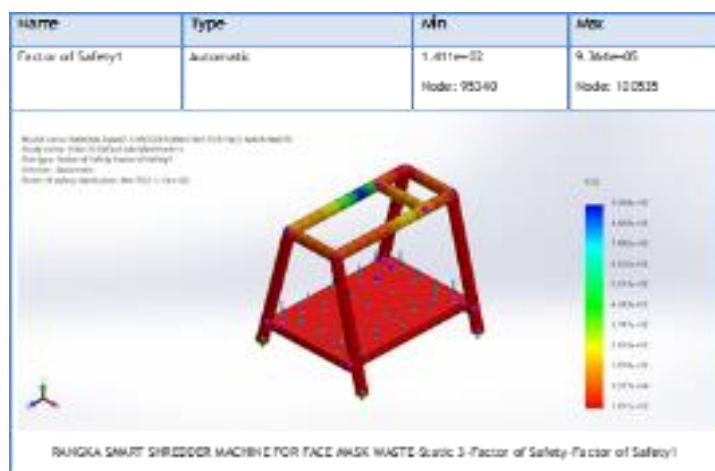


Fig. 14. The factor of safety loading 5kg on the frame.

3.2 Design Results

The Fig. 15 explains the design concept and layout using computer software, as shown in the drawings and draft ideas.



Fig. 15. Design results.

4 Conclusion

This research has produced a frame design for a mask waste shredder machine that could be applied in industrial areas. The mask waste shredder machine consisted of a shredder that functioned as a counter for mask waste until it became a certain size. By using the three-phase motors, the transmissions (clutch chain axle and pin) turn the paper crusher machine while it is turned on. In addition, all mask waste shredder machine components were supported by a hollow steel frame measuring 40×40 mm and 2 mm thick.

The simulation and test results showed that the machine could support each part of the machine when shredding mask waste up to a certain size. The enumeration process applied reverse rotation

on the driving motor. Thus, the shredder, at a certain time, rotated in the opposite direction and then back to its original rotation to shred the part of the mask that had not been completely shredded.

References

- [1] S. Saadat, D. Rawtani, and C. M. Hussain, "Environmental perspective of COVID-19," *Science of the Total Environment*, vol. 728, p. 138870, 2020, doi: 10.1016/j.scitotenv.2020.138870.
- [2] H. Harapanet *al.*, "Willingness-to-pay for a COVID-19 vaccine and its associated determinants in Indonesia," *Hum VaccinImmunother*, vol. 16, no. 12, pp. 3074–3080, 2020, doi: 10.1080/21645515.2020.1819741.
- [3] S. Sangkham, "Face mask and medical waste disposal during the novel COVID-19 pandemic in Asia," *Case Studies in Chemical and Environmental Engineering*, vol. 2, no. September, p. 100052, 2020, doi: 10.1016/j.csee.2020.100052.
- [4] World Health Organization, "Pembersihandandisinfeksipermukaanlingkungandalamkonte ks COVID-19," *Panduan interim*, pp. 1–9, 2020.
- [5] A. Hamdani, A. H.-J. of G. S. and, and undefined 2021, "The Face Mask Waste Recycling Generated During Covid-19 Pandemic In Indonesia," *Journal.Unpad.Ac.Id*, vol. 5, no. 2, pp. 31–34, 2021.
- [6] F. D. B. De Sousa, "Pros and cons of plastic during the COVID-19 pandemic," *Recycling*, vol. 5, no. 4, pp. 1–17, 2020, doi: 10.3390/recycling5040027.
- [7] M. H. Chua *et al.*, "Face Masks in the New COVID-19 Normal: Materials, Testing, and Perspectives," *Research*, vol. 2020, pp. 1–40, 2020, doi: 10.34133/2020/7286735.
- [8] A. W. H. Chin *et al.*, "Stability of SARS-CoV-2 in different environmental conditions," *Lancet Microbe*, vol. 1, no. 1, p. e10, 2020, doi: 10.1016/S2666-5247(20)30003-3.
- [9] Z. Lironget *al.*, "Aerosol and Surface Stability of SARS-CoV-2 as Compared with SARS-CoV-1," *New England Journal of Medicine*, vol. 382, no. 12, pp. 1177–1179, 2020.
- [10] W. H. Organization and M. C. Joint, "Report of the WHO-China Joint Mission on Coronavirus Disease 2019 (COVID-19)," *The WHO-China Joint Mission on Coronavirus Disease 2019*, vol. 2019, no. February, pp. 16–24, 2020.
- [11] D. Koh, "Occupational risks for COVID-19 infection," *Occup Med (Chic Ill)*, vol. 70, no. 1, pp. 3–5, 2020, doi: 10.1093/occmed/kqaa036.
- [12] A. Haryono, "UrgensiPengelolaanLimbahMedis di MasaPandemi Covid-19." Accessed: Feb. 15, 2022. [Online]. Available: <http://lipi.go.id/siaranpress/urgensi-pengelolaan-limbah-medis-di-masa-pandemi-covid-19/22339>
- [13] L. Hasibuan, "IniBahayaPakai Masker Berulang-ulangTanpaGanti."
- [14] D. H. R. Spennemann, "Covid-19 face masks as a long-term source of microplastics in recycled urban green waste," *Sustainability (Switzerland)*, vol. 14, no. 1, 2022, doi: 10.3390/su14010207.
- [15] A. Sharma and A. Kumar, "Design and Fabrication of Surgical Masks and Gloves Destroyer Machine," *International Journal of Science and Research*, vol. 10, no. 1, pp. 2319–7064, 2019, doi: 10.21275/SR21104121348.
- [16] I. Beckham, F. J. Daywin, I. W. Sukania, L. Laricha, and L. Gozali, "MODIFICATION DESIGN OF SHREDDER MASK WITH DISINFECTANT SPRAYER BY USING REVERSE ENGINEERING AND VDI 2221 METHODS," pp. 1559–1568, 2021.
- [17] Y. Yao, W. M. Quach, and B. Young, "Finite element-based method for residual stresses and plastic strains in cold-formed steel hollow sections," *EngStruct*, vol. 188, pp. 24–42, Jun. 2019, doi: 10.1016/J.ENGSTRUCT.2019.03.010.

- [18] “Yield Condition,” *Advanced Topics in Science and Technology in China*, pp. 32–63, 2009, doi: 10.1007/978-3-540-88152-0_3/COVER.
- [19] O. İnal, K. B. Katnam, J. Taylor, S. Sprenger, P. Potluri, and C. Soutis, “On the static failure behaviour of co-cured composite joints with enhanced interlaminar fracture energies via multiscale toughening,” *Compos Struct*, vol. 315, p. 116966, Jul. 2023, doi: 10.1016/J.COMPSTRUCT.2023.116966.
- [20] A. L. Muthuveerappan and S. Sivarajan, “Finite element analysis of process parameters influences on deformation and von mises stress in drilling,” *Mater Today Proc*, May 2023, doi: 10.1016/J.MATPR.2023.05.113.
- [21] S. E. Jørgensen and T. M. Swannack, “Model types: Overview,” *Encyclopedia of Ecology*, pp. 145–153, Jan. 2018, doi: 10.1016/B978-0-12-409548-9.11146-7.
- [22] X. Huang, C. Oram, and M. Sick, “Static and dynamic stress analyses of the prototype high head Francis runner based on site measurement,” in *IOP Conference Series: Earth and Environmental Science*, Institute of Physics Publishing, 2014. doi: 10.1088/1755-1315/22/3/032052.